Journal of Polymers and the Environment (2022) 30:3582–3597
https://doi.org/10.1007/s10924-022-02453-x

ORIGINAL PAPER

# Development of Hybrid Film Based on Carboxymethyl Chitosan-Gum Arabic Incorporated Citric Acid and Polyphenols from *Cinnamomum camphora* Seeds for Active Food Packaging

**Fawze Alnadari[1,3] · Anthony Pius Bassey[1] · Mohamed Abdin[1,4] · Mohamed Abdelbaset Salama[4] · Mustapha Muhammad Nasiru[1] · Zhuqing Dai[2] · Yuhang Hu[1] · Xiaoxiong Zeng[1]**

Accepted: 5 April 2022 / Published online: 30 April 2022
© The Author(s), under exclusive licence to Springer Science+Business Media, LLC, part of Springer Nature 2022

## Abstract

In this study, carboxymethyl chitosan with gum Arabic (CG) based novel functional films containing *Cinnamomum camphora* seeds extract (CCSE) at varying concentrations (0.5, 1.2 and 2% in w/w) were successfully fabricated. Moreover, sixteen phenolic compounds were identified by liquid chromatography and electrospray-ionized quadrupole time-of-flight mass spectrometry (LC-ESI-QTOF-MS) and the most abundant organic acid was citric acid (present at 1062.55 µg/g dry weight in CCSE). The resulting CG-ANC.P film was comprehensively characterized in terms of physicochemical properties, morphological characteristics, molecular properties, melting, and bioactivities properties (antimicrobial, antioxidant and biodegradability). CCSE inclusion into CG resulted in a marked increase (33.01–63.23 MPa) of tensile properties, with optimum thickness. The swelling degree, water solubility, and water vapor permeability were markedly ($p < 0.05$) reduced from 54.21 to 31.70%, 32.05 to 14.02%, and 3.46 to $1.12 \times 10^{-11}$ $g^{-1}$ $s^{-1}$ $Pa^{-1}$, respectively. The open control and CG samples showed much higher peroxide values of sunflower oil ($69.49 \pm 0.68$ and $20.15 \pm 0.31$ mEq/kg, respectively) while CG-CCSE2 exhibited a low value ($9.79 \pm 0.28$ mEq/kg) after 28 days incubation. The CG biodegradable film with the addition of CCSE (2%) was optimal for producing functional films with antioxidant and antibacterial properties.

**Keywords** *Cinnamomum camphora* · Bioactive compounds · Edible film · Antioxidant · Antimicrobial · Food packaging

## Abbreviations

| | |
|---|---|
| CCSE | *Cinnamomum camphora* Seeds extract |
| CG | Carboxymethyl chitosan with gum Arabic |
| CG-CCSE | Carboxymethyl chitosan-gum Arabic with *C. camphora* seeds extract |
| CMC | Carboxymethyl chitosan |
| EB | Elongation at break |
| GA | Gum Arabic |
| LC-ESI-QTOF-MS | Liquid chromatography coupled with electrospray-ionisation triple quadrupole time-of-flight mass spectrometry |
| POV | Peroxide value |
| TS | Tensile strength |
| WVP | Water vapor permeability |

✉ Xiaoxiong Zeng
zengxx@njau.edu.cn

1 Department of Food Science and Engineering, College of Food Science and Technology, Nanjing Agricultural University, Nanjing 210095, Jiangsu, China

2 Institute of Agro-Product Processing, Jiangsu Academy of Agricultural Sciences, Nanjing 210014, Jiangsu, China

3 Department of Food Science and Nutrition, Faculty of Agriculture, Food and Environment, Sana'a University, Sana'a, Yemen

4 Agriculture Research Center, Food Technology Research Institute, Giza 12611, Egypt

## Introduction

About 39,000–52,000 consumption of micro-plastic particles by humans is recorded annually [1]. Many environmental problems are happened due to the unending utilization of petroleum-based plastic materials because of their non-degradable nature [2]. Consequently, the accumulation of these plastic materials in landfills or oceans induces eco-pollution [3], thereby posing health risks to consumers. To ameliorate this environmental concern, new food packaging

films have been developed by researchers from various biopolymers such as polysaccharides, lipids, and proteins. Due to their suitable characteristics like vapor and water barrier [4], the potential application of these materials in food preservation as alternative packaging sources is imperative. Importantly, positive comments have been received for bio-based films as a biodegradable substance and also as a carrier of bioactive substances [2].

Green active packaging is an innovative technology that has appeared as an enticing alternative for the food packaging film, which contains bioactive compounds including antimicrobials and antioxidants [5–7]. Several natural ingredients such as tea polyphenols [8], chives root extract [9], red grape extract [10] and mango peel extract [5] have been reported to enhance the antioxidant efficacy of bio-based films. The vast amount of wastes generated from the processing of fruits and vegetables can be utilized as potential polyphenol sources and other bioactive compounds [11].

Carboxymethyl chitosan (CMC) is a promising biocompatible and biodegradable polymer produced from chitosan reaction with mono-chloroacetic acid under alkaline conditions [12]. Gum Arabic (GA), a negatively-charged heteropolysaccharide derived from the branches of Acacia tree trunks, has been distinguished as ideal for use in oil-in-water emulsion systems following its encapsulation and emulsification potentials [13–15]. Additionally, the polyelectrolytic property in the presence of uronic acid enables its use as encapsulation carriers of active components by simple or complex polyelectrolyte complexes [16]. Through electrostatic interactions, polyanionic GA can form characteristic composites with polycationic polymers like CMC, with the complexes exhibiting different behaviors in different mass ratios [17]. Though the attempt to apply CMC and GA in food packaging has been studied, their low antioxidant and antimicrobial potential make them undesirable and inefficient food packaging [18]. Therefore, to mitigate these constraints, numerous natural plants possessing potent bioactivities, including quercetin [19], propolis extract [20], pullulan [21], polyphenols extracted [22], protein isolate extracted [23], and seed cover extract [24] have been incorporated into CMC and GA film. *Cinnamomum camphora* tree belongs to the *Lauraceae* family. It is widely grown as a landscape tree in Southern China and abundant in Korea, Vietnam, Japan, and India across tropical and subtropical zones. *C. camphora* seeds are abundant, with a yearly yield exceeding 1 million tons in China [25]. The seeds of the tree are not only used for oil extraction but also to treat various ailments [26]. The health benefits and biological functions of *C. camphora* seeds are mostly associated with their polyphenolic contents [27]. Previous studies have also indicated that *C. camphora* seeds consist of approximately 58.02% crude fat, 18.15% crude protein, 17.9% carbohydrate, 3.97% moisture, and 1.96% ash [25]. In China, the seeds are often used in almost every extraction of oil and traditional Chinese medicine, thereby generating huge residues in the form of seeds [28]. The polyphenols of *C. camphora* seeds extract (CCSE) have also been known to possess antimicrobial and antioxidant properties [29]. Therefore, liquid chromatography and electrospray-ionized quadrupole time-of-flight mass spectrometry (LC-ESI-QTOF-MS) was applied to identify polyphenols and organic acids in CCSE. Sixteen phenolic compounds were identified, and the most abundant phenolic compounds were 4-hydroxybenzoic acid and *p*-coumaric acid. Due to this, the exploration of CCSE as a potent component for developing carboxymethyl chitosan with gum Arabic (CG)-based active packaging film should be considered. Thus, this study was designed to explore the effect of CCSE as an active ingredient to produce CMC with GA active food packaging film and to estimate the structural, mechanical, biological and physical activities of the produced films. Furthermore, the produced film was examined as a potential packaging material for oil storage in the food industry.

## Materials and Methods

### Materials and Reagents

The seeds of *C. camphora* were collected in the ripening stage from the trees growing at Nanjing Agricultural University (Nanjing, China). Analytical grade standards of protocatechuic acid, gentisic acid, phlorizin, 4-hydroxybenzoic acid, procyanidin B3, citric acid, *p*-coumaric acid, syringic acid, L-ascorbic acid, ferulic acid, caffeic acid, salicylic acid, quercetin, rutin, catechin and epicatechin were purchased from Henan Putian Tongchuang Biotechnology Co., Ltd. (Henan, China). CMC (MW 260 kDa) with 80% degree of substitution was purchased from Macklin Biotechnology Co. Ltd. (Shanghai, China). GA (MW 250 kDa) was obtained from the Shanghai Ryon Biological Technology Co., Ltd. (Shanghai, China). Glycerol was obtained from Guangdong Guanghua Sci-Tech Co., Ltd. (Guangdong, China). D101 macroporous resin was purchased from the Chemical Plant of Nankai University (Tianjing, China). 2,2-Diphenyl-1-picrylhydrazyl (DPPH) and 2,2′-azino-bis-(3-ethylben-zothiazoline-6-sulphonic acid) (ABTS) were obtained from Sigma Chemical Co., Ltd. (St Loius, MO, USA). Gallic acid was purchased from Aladdin Industrial Inc. (Shanghai, China). The sunflower oil was obtained from a local market (Nanjing, China,). All other reagents used were of analytical grade.

## Preparation and Purification of CCSE

The seeds were peeled from fresh *C. camphora* fruits and oven-dried for 12 h at 50 °C. The crushed seeds (25 g) were continuously extracted with 150 ml of petroleum ether at 45 °C for 6 h in a Soxhlet apparatus to remove oil. Subsequently, the crushed seeds were ground to powder, then extracted by impregnation with an aqueous ethanol solution (80%) at 45 °C for 90 min, with ultrasonication at 300 W (KQ 300DB, 300 W, 0–40 kHz, Kunshan Ultrasonic Instrument, Kunshan, China). The supernatants were collected after vacuum filtering and concentrated at 45 °C using a vacuum rotary evaporator. The resulting aqueous extract was loaded onto a column (5 × 30 cm) of D101 macroporous resin. The strong polar constituents were firstly removed with distilled water, and the target constituents were eluted with ethanol (80%) at a flow rate of 1.5 ml/min. The obtained purified crude CCSE extract was freeze-dried in a vacuum freeze dryer.

## Characterization of Phenolic Compounds in CCSE

### Total Phenolic Content

The Folin-Ciocalteu method outlined by Islam et al. [30] was adopted to evaluate the total polyphenol content of CCSE. Briefly, 0.5 ml from the sample was added to 1.0 ml from the reagent (Folin-Ciocalteu) was diluted 10 times and left in the dark for 6 min. After that, 2.5 ml from $Na_2CO_3$ (75 g/L) was added and the mixture was kept for 30 min at 25 °C. At 765 nm, the absorbance of the sample was measured, and the amount of total phenolic content was expressed as mg of gallic acid equivalent (GAE) per g of extract. Gallic acid was used as a standard for plotting the calibration curve. All experiments were repeated six times.

### LC-ESI-QTOF-MS Analysis

Identification and quantification of polyphenols in CCSE were achieved by the LC-ESI-QTOF-MS system (G2-XS QTOF Waters, Manchester, UK). In brief, the extract was prepared at a concentration of 5 mg/ml. After that, the samples were centrifuged at 3000 rpm (Beckman coulter Avanti J-265XP) for 15 min at 2 °C. Continuously, 1.5 ml of supernatants were collected in HPLC vials for LC–MS, and 2 µL solution was injected into the UPLC column (2.1 × 100 mm, 1.7 µm particles, ACQUITY UPLC BEH C18 column) with a flow rate of 0.3 ml/min. Buffer A consisted of 0.1% formic acid in the water, and buffer B consisted of 0.1% formic acid in acetonitrile. The gradient was 5% Buffer B for 0.5 min, 5–95% buffer B for 11 min, 95% buffer B for 2 min. Electrospray ionization (ESI) was used as a source in positive modes with a preferred mass spectrum in the *m/z* range 100–1600. The leucine-enkephalin (*m/z* 556.2771) was used for recalibration and removing the lock mass. Ionization parameters were the following: the capillary voltage was 2.5 kV, sample cone was 40 V, source temperature was 120 °C and desolvation gas temperature was 800 °C. Data acquisition and processing were performed using Masslynx software version 4.1.

### HPLC Analysis of CCSE

Aglient 1100 Series HPLC system (USA) with DAD detector and Phenomenex SynergiTM 4 µm RP-Hydro C-18 (0.46 × 250 mm) was used to determine the phenolic composition of CCSE. Two mobile phases were used, formic acid in deionized water 0.1% (v/v) (A) and acetonitrile (B). The flow rate was set at 15–30% from 0 to10 min, 30–50% from 10 to15 min, 50–60% from 15 to 20 min, and 60–70% from 20 to 25 min, and 70–80% from 25 to 30 min. The injection volume and the flow rate were 20 µL and 0.35 ml/min, respectively. The samples were measured at 280 nm and the column temperature was 35 °C.

## Preparation of Films

The films were fabricated by dissolving 6.0 and 3.2 g of CMC and GA, respectively, in distilled water (400 ml). After stirring (800 rpm, 60 °C, 2 h), the glycerol solution (35% w/w based on CMC and GA used), used as a plasticizer, was added to the mixture and thoroughly homogenized by stirring at 800 rpm at 50 °C for 30 min. After that, CCSE was added at the concentration of 0, 0.5, 1.2 and 2% (based on CMC and GA used) to afford groups of CMC/GA (CG, control), CMC/GA with the respective concentrations denoted as (CG-CCSE 0.5, CG-CCSE 1.2, and CG-CCSE 2), respectively. Every group was stirred (40 °C, 800 rpm, 1 h) to afford a thorough blend. Afterward, 50 ml aliquot from each group was carefully poured into petri-dish plates (150 mm) and oven-dried (45 °C, 12 h). The films were then peeled off the plates and stored in a desiccator at 30 °C until further analysis.

## Characterization and Mechanisms of Films

### Scanning Electron Microscopy (SEM) Analysis

The film samples (2 × 2 mm) were mounted on a bronze stub and sputtered with a thin layer of gold. The surface and cross section morphology of the film samples were observed by using a SEM (SU8010, Hitachi, Japan) with an acceleration voltage of 10 kV.

#### Fourier Transform-Infrared Spectroscopy (FT-IR) Analysis

FT-IR spectrometer (Nicolet iS-50, Thermo Fisher Scientific, MA, USA) was used to characterize the presence of functional groups in the powder of CMC, GA and CCES and film samples. The spectra were collected in a wavelength range of 4000–525 $cm^{-1}$ by averaging 32 scans at a resolution of 4 $cm^{-1}$.

#### X-ray Diffraction (XRD)

An X-ray diffractometer (D8 Advance, Bruker, USA) was used to identify the crystal structure of the films at 30 kV and 10 mA. Angular range (2θ = 5 – 80 degrees) was applied to detect the scattered radiation at 15.6 degrees/min scanning speed.

#### Differential Scanning Calorimetry (DSC) Analysis

DSC (DSC-60, Shimadzu Corp., Kyoto, Japan) was used to analyze the thermal properties of the films. Briefly, 10 mg of film pieces were sealed in a standard aluminum pan which was heated under a nitrogen atmosphere from 27 to 450 °C at a rate of 10 °C/min.

#### Thickness and Mechanical Properties Analysis

The film thickness was estimated by a digital hand-held micrometer (Mitutoyo Absolute, Tester Sangyo Co. Ltd., Japan). Each sample was measured 10 times randomly at various levels, and the mean was calculated. Additionally, a texture analyzer (TA.XT Plus, Stable Micro Systems Ltd., Surrey, UK) was employed to analyze the mechanical properties (tensile strength percentage (TS) and elongation-at-break (EB) of the films at room temperature. Film strips (10 × 80 mm) were positioned on grips (50 mm) with the tensile power and cross speed processed at 5 kN and 50 mm/min, respectively. The films were examined three times. TS and EB values, per the values of extensibility (mm) and resistance to extension (N), were calculated using the equation.

$$TS(MPa) = \frac{F}{X \times W} \times 100 \quad (1)$$

$$EB(\%) = \frac{\Delta L}{L} \times 100 \quad (2)$$

where $F$ = resistance to extension ($N$), $X$ = film thickness (mm) and $W$ = the width of the film (mm), $\Delta L$ = the increase in the distance at the break (mm) and $L$ = the original length between grips of the film (mm).

#### Measurements of Solubility, Swelling Ratio and Moisture

The film bands (20 × 20 mm) were weighted as wet weight ($M_0$) and dried at 105 °C till constant weight to calculate the primary dry mass value ($M_1$). The dried pieces were transferred to 100 ml beakers filled with distilled water (50 ml) covered with plastic wraps and preserved at 25 °C for 24 h. Next, the films were dehydrated superficially with filter papers and weight to get ($M_2$). The saturated-hydrate films were dehydrated again to constant weight at 105 °C to afford final dry mass ($M_3$). The moisture content (MC), swelling ratio, and solubility were measured using the equation below.

$$\text{Moisture content}(\%) = \frac{M_0 - M_1}{M_0} \times 100 \quad (3)$$

$$\text{Sweling ratio}(\%) = \frac{M_2 - M_0}{M_0} \times 100 \quad (4)$$

$$\text{Film solubility}\ (\%) = \frac{M_1 - M_3}{M_1} \times 100 \quad (5)$$

where $M_0$ = initial weight of the film, $M_1$ = initial dry weight of the film, $M_2$ = weight after drenching films in water for 24 h, and $M_3$ = dry weight of the film after drenching films in water for 24 h.

#### Analysis of Water Vapor Permeability (WVP) of Films

The method of Zhang et al. [31] was followed to estimate the WVP values of the films with minor changes. The film samples (5 × 5 cm) and anhydrous $CaCl_2$ were loaded in special glass cups (4 cm) and sealed. After that, the cups were placed in a desiccator at 75% humidity and packed with sodium chloride saturated solution. Thereafter, for 10 h, the weight of the cups was recorded each hour and after 24 h. By using linear regression, the slope of weight difference against time was recorded against time. The WVP (g $m^{-1}$ $s^{-1}$ $Pa^{-1}$) was estimated as follows:

$$\text{WVP} = \frac{\text{Slope} \times L}{A \times \Delta P} \quad (6)$$

where $L$ = average film thickness (m), $A$ = transfer area ($m^2$), and $\Delta P$ = difference in the pressure of partial water vapor.

### Film Color and Opacity

The color of films was measured using a colorimeter (CR-40, Minolta, Camera Co., Japan) with illuminant D65, a 0 degree viewing angle, and a 0.13 mm diameter viewing area was used to determine the color of prepared films. Before measurement, the Colorimeter was calibrated with a white tile (mod CR-A43). The equations below were used to estimate the total color variation (ΔE), white (WI) and yellow (YI) indexes.

$$\Delta E = \left( \left( L_i^* - L^* \right)^2 + \left( a_i^* - a^* \right)^2 + \left( b_i^* - b^* \right)^2 \right)^{1/2} \quad (7)$$

$$YI = \frac{142.68 \times b^*}{L^*} \quad (8)$$

$$WI = 100 - \left( (100 - L^*)^2 + a^{*2} \right)^{1/2} + b^{*2} \quad (9)$$

UV-722 spectrophotometer (Shanghai Jinghua Science & Technology Instruments Co., Ltd., China) was used to determine the opacity of the samples at 600 nm. The transparency for the sliced bands (80 × 45 mm length) was assessed. The opacity was calculated as equated below.

$$\text{Opacity} = \frac{A}{L} \quad (10)$$

where $A$ = absorbance value at 600 nm and $L$ = film thickness (nm).

### Determination of the Antioxidant Activity of Films

The method outlined by Abdin et al. [32] was employed to determine the antioxidant activity of the films. Each film sample (25 mg) was added to a test tube including 3.0 ml of distilled water and kept at 37 °C for 6 h with gentle shaking to release the extract. The extract solution (50 µL) was mixed with 200 µL of working solution from ABTS, the absorbance at 734 nm was measured, and scavenging activity was estimated as shown below.

$$\text{Scavenging activity on ABTS free radicals (\%)} = \left( 1 - \frac{A_1 - A_2}{A_0} \times 100 \right) \quad (11)$$

where $A_0$ = $ABTS^+$ initial absorbance, $A_1$ = sample absorbance, and $A_2$ = sample with PBS absorbance.

To determine the DPPH radical scavenging activity, 50 µL from the extract solution was blended with 200 µL of DPPH methanolic solution (0.2 mM) and put in the dark for 30 min at 30 °C. Later, the absorbance was measured at 517 nm with ascorbic acid used as the control. The scavenging activity was calculated as follows.

$$\text{Scavenging activity on DPPH free radicals (\%)} = \left( 1 - \frac{A_1 - A_2}{A_0} \times 100 \right) \quad (12)$$

where $A_0$ = initial DPPH absorbance, $A_1$ = sample absorbance, and $A_2$ = sample absorbance with water.

### Assay of Antimicrobial Activity of Films

The procedure of Khalid et al. [33] was employed to evaluate the antimicrobial activity of the prepared films against Gram-negative (*Escherichia (E.) coli* CGMCC 1.8721) and two Gram-positive *(Staphylococcus (S.) aureus* (CGMCC 1.8721) and *Bacillus (B.) cereus* (CGMCC 1.895)) bacteria. Briefly, each bacterial culture was diluted to afford a final $10^5$ CFU/ml concentration. The cells (0.1 ml) were spread onto a new medium agar plate. Subsequently, the discs of films (12 mm diameter) were prepared, sterilized under UV light, placed carefully in petri-dish plates, and incubated (37 °C, 24 h). A sliding caliper was used to estimate the area of the inhibitory zones.

### Biodegradation Test

The composting test described by Tan et al. [34] was adopted to analyze the biodegradation capacity of the prepared films. Briefly, the soil was collected from the experimental area at Nanjing Agricultural University (Nanjing, China). It was then put in a tray made from plastic and buried with the films (2 × 2 cm) at 4 cm depth for 21 days. The soil was treated twice daily with water. Each week, the films were removed and their weight loss calculated using the following equation:

$$\text{Weight loss(\%)} = \frac{M_0 - M_1}{M_0} \times 100 \quad (13)$$

where $M_0$ = initial film weight and $M_1$ = film weight after 7, 14, or 21 days of biodegradation.

## Experiments of Packaging of Sunflower Oil

### Capability of Films for Oil Resistance

The procedure of Wang et al. [35] was adopted to determine the capability of films for oil resistance with minor changes. Briefly, Whatman No. 1 filter paper (6 cm diameter) was dried in the hot-air oven at 50 °C. The films (4 × 4 cm) were then fitted with ropes above 5 cm of oil-containing glass test tubes and positioned downward for 48 h on the filter paper. Afterward, the weight was recorded, and the oil absorption ratio (OAR) was measured.

$$OAR(\%) = \left(\frac{m}{m_0} - 1\right) \times 100 \quad (14)$$

where $m$ = the weight of filter paper after 48 h and $m_0$ = weight of dried filter paper.

### Determination of Peroxide Value (POV)

Sunflower oil (10 ml) was added into a glass test tube (15 × 150 mm) and samples containing sunflower oil were sealed and stored for 28 days at 50 °C. From each sample, 10 ml was taken on days 1, 7, 14, and 28 to determine the POV by iodometric titration as outlined by the National Standard of the People's Republic of China GB/T5009.227–2016 [36] with slight changes. Briefly, sunflower oil (7.0 ml) was dissolved in 30 ml of 2:3 (v/v) acetic acid and trichloromethane before adding 1.0 ml saturated potassium iodide and shaken in the dark for 1 min. Afterward, distilled water (30 ml) was added and shaken for 1 min before adding starch indicator (1%, 0.5 ml) into the mix. The solution was titrated with 0.01 N sodium thiosulfate until the blue color disappeared, and the consumption rate was recorded. POV (mEq/kg) was calculated as shown below:

$$POV(mEq/kg) = \frac{V \times N \times 1000}{W} \quad (15)$$

where $V$ = volume of sodium thiosulfate for titration (ml), $N$ = normality of thiosulfate, and $W$ = weight of the lipid (g).

### Statistical Analysis

The film properties were measured in triplicate with individually prepared films as replicated experimental units. All data were statistically analyzed using statistical software SPSS 16.0. To assess the difference between factors and levels, one-way Analysis of variance (ANOVA) was applied. Duncan multiple range tests were used to determine the significant differences ($p < 0.05$) between means.

## Results and Discussion

### Characterization of Phenolic Compounds

The total phenolic content of *C. camphora* seeds was 40.16 ± 1.44 mg of GAE/g of extract. The *C. camphora* seeds extract showed a fair amount of phenolic content, which is consistent with previous results [27, 29]. Moreover, citric acid and *4*-hydroxybenzoic acid were mainly in CCSE. This observation also supported the results of LC-ESI-QTOF-MS. These observations illustrate that seed waste is a valuable source of citric acid that can be used not only to increase bioactivity but also to generate biodegradable food packaging films based on CG.

Untargeted qualitative analysis of phenolic compounds in CCSE was done by LC-ESC-QTOF/MS. Polyphenols in both positive and negative ionization modes were tentatively described based on their *m/z* value from MS spectra. Table 1 displays all the compounds found in the seeds extract of *C. camphora*. A total of 16 phenolic compounds and citric acid were identified in *C. camphora* seeds (Table 1), they were mainly phenolic acids (8) and flavonoids (6) followed by other polyphenols, including hydroxycinnamic acids, hydroxybenzoic acids, flavones and flavanols. CCSE displayed citric acid and two polyphenolic compounds (4-hydroxybenzoic and *p*-coumaric acids) which lead to variation in organic acids, flavonoids, phenolic acids, other polyphenols and overall antioxidant activity [27, 29].

### Characterization of Films Properties

#### Observation of Film Microstructure by SEM

The surface images and cross-sections of control and CCSE-treated films were screened (Fig. 1A and B). The SEM images indicated that gum Arabic surfaces in the composite film impacted the arboxymethyl chitosan structure in the CG control film, causing discontinuities in the matrix of the polymer, indicating that the surface roughness of the film was increased. However, at a low concentration of compounds from CCSE extract, CG-based films incorporated with CG-CCSE 0.5% formed a uniformly dispersed film with aggregation, while CCSE at high concentrations (1.2 and 2%) the surface became more homogenous, indicating that the fillers are compatible with the polymer matrix with potentially good adhesion, intermolecular binding, and affinity between the filler and the polymer matrix [37]. Consequently, the presence of compounds from CCSE extract enhanced the smoothness, uniformity, and homogeneity in the structures without any apparent defects. Besides, SEM images of the cross-section of the CG-CCSE-based composite film (CG-CCSE 2%) showed that no voids were present

**Table 1** Identification and quantification of compounds from CCSE extract by using LC-ESI-QTOF-MS

| No | Name of compound | Retention time (tr/min) | [M-H] − m/z | [M + H] + m/z | Calibration equation | Regression coefficient ($R^2$) | Content (µg/g dw) |
|---|---|---|---|---|---|---|---|
| 1 | Procatechuic acid | 2.31 | 153.0188 | 155.0345 | γ = 16055x + 15,230 | 0.998 | −35 |
| 2 | Catechin | 3.86 | 289.0712 | 291.0869 | γ = 34984x + 78,939 | 0.9932 | −86.52 |
| 3 | Caffeic acid | 4.45 | 179.0344 | 181.0501 | γ = 31698x + 30,606 | 0.9907 | −34.56 |
| 4 | Epicatechin | 5.24 | 289.0712 | 291.0869 | γ = 34400x + 40,232 | 0.9907 | −42.83 |
| 5 | Ferulic acid | 7.13 | 193.05 | 195.0657 | γ= 14744x + 9076.8 | 0.9923 | −18.85 |
| 6 | Ferulic acid isomer | 3.41 | 193.05 | 195.0657 | γ = 14744x + 9076.8 | 0.9945 | −3.33 |
| 7 | Rutin | 7.67 | 609.1456 | 611.1612 | γ= 41507x + 32,683 | 0.9969 | −20.88 |
| 8 | Salicyclic acid | 8.93 | 137.0239 | 139.0395 | γ = 28337x + 15,500 | 0.9991 | −21.03 |
| 9 | Citric acid | 0.99 | 191.0192 | 193.0348 | γ = 5970.9x − 545.05 | 0.994 | 1062.55 |
| 10 | 4-hydroxybenzoic acid | 3.52 | 137.0239 | 139.0395 | γ = 8136.4x + 6108.1 | 0.997 | 19.02 |
| 11 | Procyanidin B3 | 3.48 | 577.1346 | 579.1503 | γ = 27220x + 28,992 | 0.9956 | −23.53 |
| 12 | P-coumaric acid | 6.16 | 163.0395 | 165.054 | γ= 21382x + 20,278 | 0.9942 | 6.62 |
| 13 | Phlorizin | 10.56 | 435.1291 | 437.1448 | γ = 27330x + 25,878 | 0.9993 | −29.72 |
| 14 | Chlorogenic acid | 3.85 | 353.0893 | 355.1029 | γ = 31698x + 30,606 | 0.9927 | −37.48 |
| 15 | Sinapic acid | 4.04 | 223.0565 | 225.0722 | – | – | – |
| 16 | Feruloylquinic acid | 7.7 | 337.0922 | 339.1079 | – | – | – |
| 17 | Morin | 9.06 | 301.0348 | 303.0503 | – | – | – |

(Fig. 1B) in the nanocomposite films and the fillers were distributed evenly in the polymer matrix (Fig. 1C). The result indicated high compatibility between the filler and the biopolymer matrix, and as a result, the intermolecular bonds between them were expected to increase [38]. Therefore, CG-based films incorporated with compounds from CCSE extract formed a uniformly dispersed film without aggregation, indicating that the fillers are compatible with the polymer matrix with potentially good adhesion, intermolecular binding, and affinity between the fillers and the polymer matrix. The attained results were comparable to the findings reported by Cheng et al. [39] and Dou et al. [40] when CG and sodium alginate films were prepared combined with different phenolic extracts.

### FT-IR Observation

Figure 2 shows the FT-IR spectra of CCSE, CMC, GA, and CG biocomposite films, and CG biocomposite films incorporated with different concentrations of compounds from CCSE extract. In the case of CCSE, a characteristic peak observed at 3243 $cm^{-1}$ was due to the O–H stretching vibration of phenol, and the peaks at 1609.78 and 1177.81 $cm^{-1}$ represented COO- (symmetric) and C–O–C stretching, respectively [21]. In the case of CMC, broadband near 1590 $cm^{-1}$ was designated to the N–H bending vibration overlapping the amide II vibration [41]. The bands observed at 1419 and 1053 $cm^{-1}$ were due to the scissoring vibrations of $NH_2$ group and the stretching vibration of C–O–C of glycosidic linkage of the polymer [42]. The GA exhibited almost the same spectra as the CG and CG-CCSE films due to the similarity of polysaccharide structure [37]. However, the addition of GA and glycerol to CMC (to form CG control film) caused shifting in wavelength values compared with GA (3287 $cm^{-1}$) to create a tough absorption band at 3276 $cm^{-1}$ for O–H stretching. The wide bond around 3276 $cm^{-1}$ was attributed to the free and stretching vibration of inter- and intra- molecular hydroxyl groups. Additionally, a new peak (2878 $cm^{-1}$), which did not appear in the CMC or GA spectrum, indicated a potential occurrence of a cross-linked reaction between CMC and GA. After CCSE addition, the peak shifted slightly from 3277 to 3282 $cm^{-1}$, which suggested that interaction existed between the surface hydroxyl groups of CCSE and the hydroxyl groups of CG molecules. Notably, the FT-IR results showed that there was no significant change in the functional groups of the composite film as compared to the CG control film, indicating that the chemical structure of the CG was not changed after incorporation of the filler. It was probably due to covalent interactions such as van der Waals and hydrogen bonding between the filler and the biopolymer matrix [38]. Collectively, these findings indicated that the incorporation of CCSE compounds into the CG films was useful for enhancing the mechanical and barrier properties of the biocomposite films.

### Observation by XRD

For the evaluation of the crystalline structure and effect of CCSE inclusion in CG film, XRD analysis was employed. As observed, CG possessed an amorphous structure with

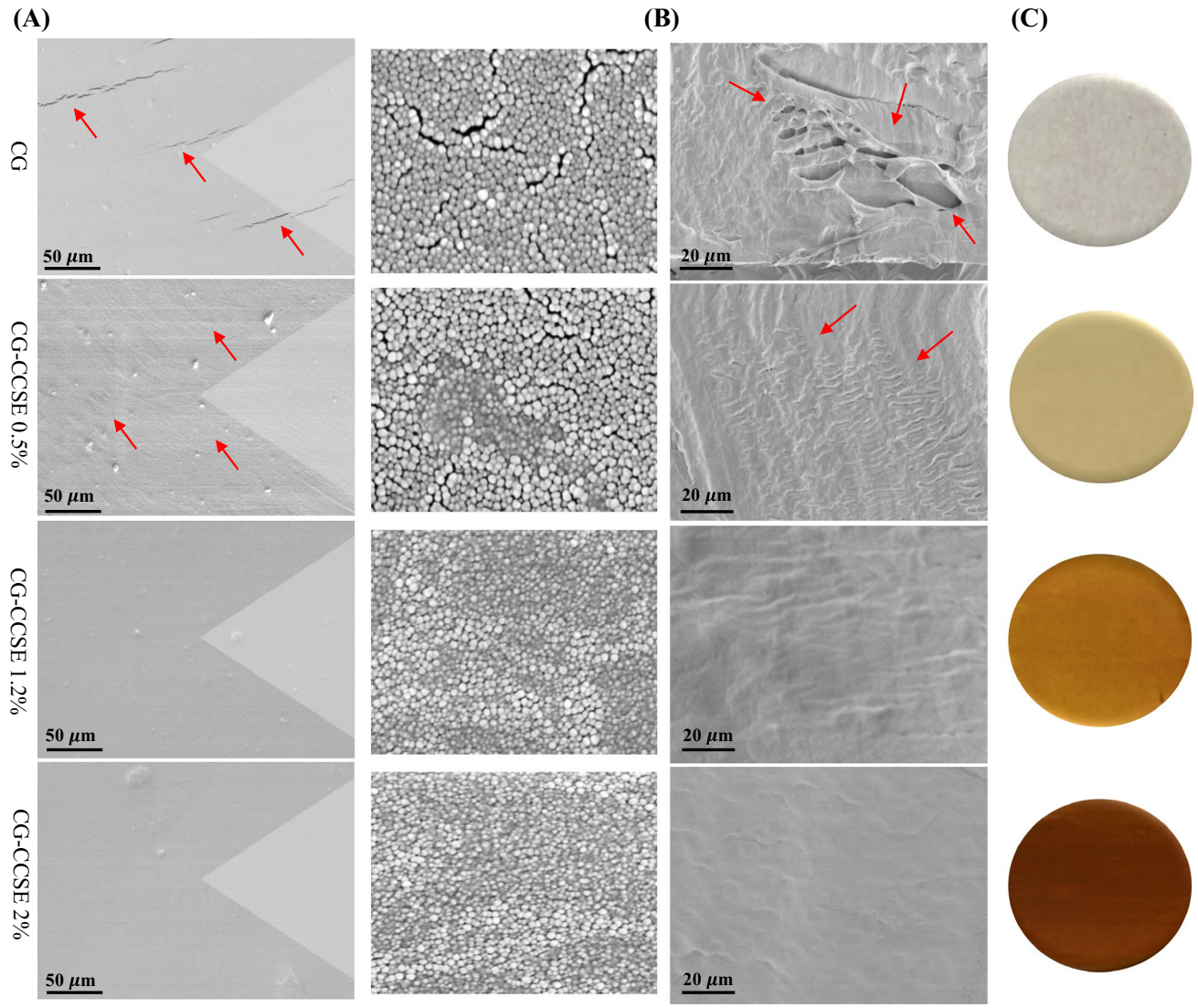


**Fig. 1** **A** Surface-sectioned SEM, **B** Cross-sectioned SEM, **C** Graphics of CG-CCSE films

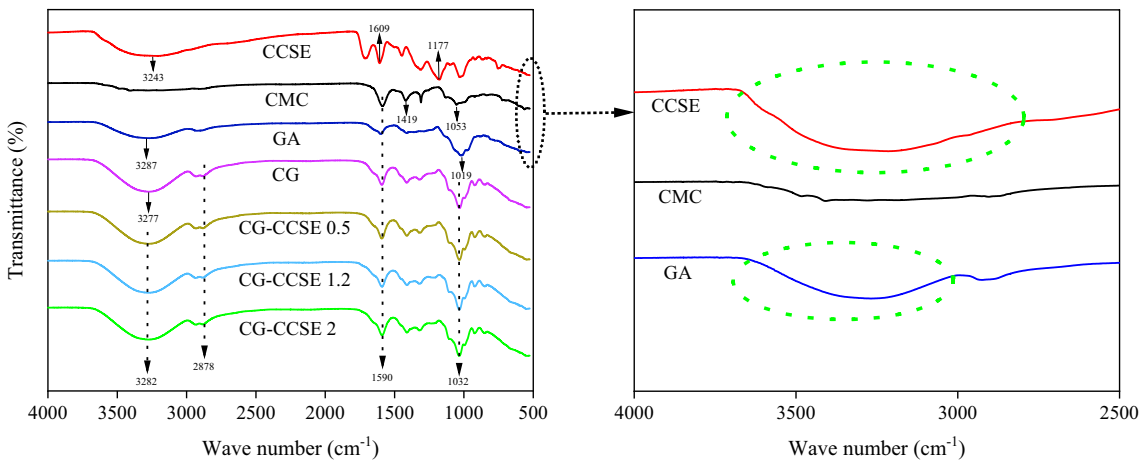


**Fig. 2** FT-IR spectra of CCSE, GA, CMC and CG-based films with different concentrations of CCSE

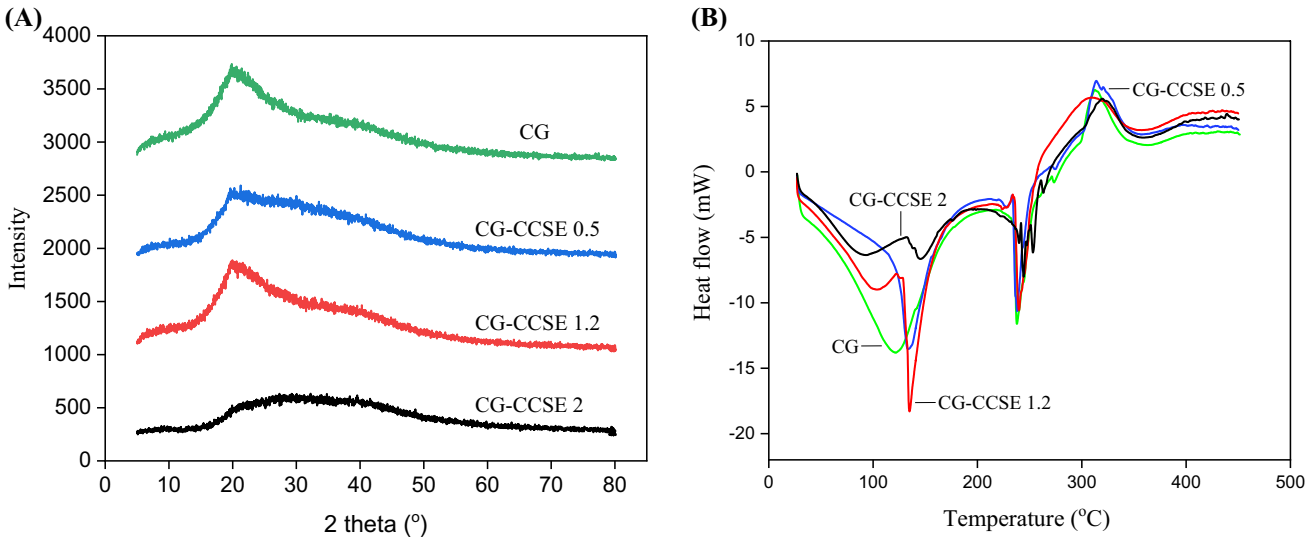


**Fig. 3** **A** X-RD pattern of CG-CCSE films, **B** DSC thermograms CG-CCSE films

a wider and single peak at 2θ about 20 degrees (Fig. 3A), corroborating the findings of Wu et al. [21]. This indicated that CCSE incorporation did not affect the inner structure of the CG control films. Also, the X-ray spectrum of films following CCSE inclusion only reduced the strength of spectral peaks, being wider with increasing CCSE concentration. This phenomenon was aided because the interaction between CG and CCSE facilitated the formation of hydrogen bonds in CG, causing a decline in crystallinity. Therefore, the mechanical characteristics of a film depend significantly on the crystallites in its structure. Similarly, Riaz et al. [43] discovered the crystallinity of carboxymethyl cellulose film raised after adding polyphenols from Chinese chives (*Allium tuberosum*), which could be connected with the retrogradation of carboxymethyl cellulose that appeared through film preservation. In CG-CCSE films, because of the competitive effect of hydrogen bonds between CG and CCSE, their interactions could hinder the formation of inter-and intramolecular hydrogen bonds in CG, thereby inducing a decline of crystallinity. These findings were consistent with a recent study [32].

### DSC Analysis

As displayed in Fig. 3B, DSC analysis was performed to determine the treated film thermal transition, and evaluate the possible changes in the film crystallinity. Except for CG-CCSE 2, which exhibited four peaks, the rest showed three distinct peaks, indicating endothermic and exothermic occurrences. As the temperature increased, a complex endothermic and exothermic behavior was visible with three distinct peaks. The first endothermic peaks (119.48 and 240.12 °C) were attributed to the loss of the residual moisture in the CG film due to heat absorption by the film, whereas the exothermic region around 311.74 °C was attributed to the breakdown and degradation of polysaccharide [44]. For the CG-CCSE 2, 148.40, 245.48 and 256.20 °C were endothermic peaks, respectively. This finding also confirmed the strong thermal stability of CG-CCSE films compared with the control film, especially the first endothermic peak (98.5 °C) when the concentration was 1.2%. Consequently, CCSE treatment could alter the structural arrangement between GA and CMC polymers. The treated films also showed a reduction in the temperature of the peak as the peak area increased. Likewise, the increase in DSC values of CG-CCSE films also corroborated the increase of the citric acid and polyphenols thermal stability. Wang et al. [45] reported that gelatin film mixture added with anthocyanins could yield tough gelatin and gelatin matrix between the anthocyanins and polymer molecules, which escalated the dissimilate temperatures and enhanced the thermal sturdiness of the films. The finding of DSC implied that the thermal stability of CCSE films in the CG matrix was concentration-dependent.

## Physical Properties of CG-CCSE Film

### Thickness

As presented in Table 2, the inclusion of CCSE did not affect the thickness of the CG films. However, it enhanced the soft elasticity and tensile strength of the films. This might be due to the interactions between polyphenols and CG, CG, which caused a tighter binding of polyphenols and CG [9]. Therefore, following the incorporation of

**Table 2** Thickness and mechanical property of CG-based CCSE films

| Film sample | Thickness (mm) | Tensile strength (MPa) | Elongation Break (%) |
|---|---|---|---|
| CG | $0.025 \pm 0.0029^{a}$ | $33.01 \pm 0.48^{d}$ | $37.24 \pm 0.92^{d}$ |
| CG-CCSE 0.5 | $0.024 \pm 0.003^{a}$ | $37.54 \pm 1.10^{c}$ | $44.06 \pm 0.60^{c}$ |
| CG-CCSE 1.2 | $0.026 \pm 0.0028^{a}$ | $54.50 \pm 0.20^{b}$ | $57.38 \pm 1.94^{b}$ |
| CG-CCSE 2 | $0.024 \pm 0.00067^{a}$ | $63.23 \pm 0.91^{a}$ | $70.03 \pm 0.69^{a}$ |

Values are expressed as mean ± standard deviation. Different letters in the same column indicate significant differences ($p < 0.05$)

CCSE into the CG film, nanoscale-quasi were produced following the continuous stirring with CCSE (0.5, 1.2 and 2.0%) addition and the interruption of the organized structure of the CG film matrix [46]. The polyphenol and CG interaction (including hydrophobic force and hydrogen bonding) increased and caused the tighter polyphenol-matrix binding, thereby inducing the compartment of the film structure and enhancing surface smoothness. This phenomenon also supported the results of SEM and mechanical properties.

### Mechanical Property of CG-CCSE Film

The mechanical property results for all the studied films are represented in Table 2. In all of the checked films, the values of tensile strength percentage (TS) and elongation-at-break (EB) were increased ($p < 0.05$). However, the CG control film showed low mechanical properties strength, and the mechanical properties of the CG control film were boosted by the inclusion of CCSE in the CG matrix. EB and TS results of CG control films were 37.24% and 33.01 MPa, while for CG-CCSE 2, they were stated to be 70.03% and 63.23 MPa, respectively. The increased TS and EB in CG-CCSE films were due to abundant hydroxyl groups in citric acid and polyphenols that could form hydrogen bonds with the hydroxyl groups in CMC/GA, resulting in stronger interfacial adhesion between CG and CCSE [47]. Similar findings have previously been published [4, 45]. On the other hand, intra-molecular forces, polymer composition, and the existence of crystallites beside the film network microstructure strongly rely on the mechanical property of a film [48]. It was apparent from the film SEM analytic results that an increase in CCSE concentration in the CG matrix led to the high homogeneity in the structure of CG control films, facilitating the strong interaction through hydrogen or ionic bonds within the CMC molecule and between GA and CCSE molecules [46]. Consequently, it could be assumed that CCSE inclusion promoted crystallinity and allowed the interchain interaction of CG, which resulted in EB and TS increase of the CCSE films.

### Moisture Content, Water Solubility, and Swelling Degree

The films water resistance behavior is significantly induced by the increase and decrease of swelling and water solubility, respectively [49]. The high solubility of CG in water makes it unfeasible to be used as a food packaging material. Hence, the incorporation of CCSE enhanced its water-resistant property. As presented in Table 3, a decline ($p < 0.05$) in water solubility and swelling was observed in CG-CCSE films. Hydroxyl groups (hydrophilic groups) in the CG molecule were integral for its intrinsic swelling behavior [33]. From the result, it is evident that the decrease in water solubility of CG-CCSE films was dose-dependent. This could be clarified due to the generation of powerful hydrogen bonds between the CG matrix and polyphenolic compounds. It was apparent that higher CCSE concentration decreased the water solubility of CG-CCSE films. Consequently, due to a decrease in water molecules linked with CG, the amount of water became less. These results supported the finding reported by Uranga et al. [50] and Rui et al. [51].

**Table 3** Physical properties of CG-based CCSE films

| Film sample | Swelling degree (%) | Solubility (%) | Moisture content (%) | WVP ($\times 10^{-11}$ $g^{-1}$ $s^{-1}$ $Pa^{-1}$) |
|---|---|---|---|---|
| CG | $54.21 \pm 6.21^{a}$ | $32.05 \pm 0.45^{a}$ | $16.92 \pm 0.33^{a}$ | $3.46 \pm 0.01^{a}$ |
| CG-CCSE 0.5 | $47.66 \pm 5.41^{a}$ | $25.54 \pm 0.51^{b}$ | $14.46 \pm 0.17^{b}$ | $2.37 \pm 0.01^{b}$ |
| CG-CCSE 1.2 | $42.53 \pm 1.88^{a, b}$ | $17.69 \pm 0.62^{c}$ | $12.70 \pm 0.50^{c}$ | $1.67 \pm 0.03^{c}$ |
| CG-CCSE 2 | $31.70 \pm 1.25^{b}$ | $14.02 \pm 0.38^{d}$ | $10.97 \pm 0.30^{d}$ | $1.12 \pm 0.02^{d}$ |

Values are expressed as mean ± standard deviation. Different letters in the same column indicate significant differences ($p < 0.05$)

### Water Vapor Permeability (WVP)

The WVP of CG-CCSE-based films are also presented in Table 3. The WVP of the CG control film was $3.46 \times 10^{-11}$ g/m/s/Pa, which is consistent with previously reported [43]. The addition of CCSE significantly decreased the WVP to 2.37 and $1.12 \times 10^{-11}$ g/m/s/Pa for the CG-CCSE 0.5% and CG-CCSE 2% composite films, respectively. The decrease in the WVP of the CG-CCSE-based composite films was mainly due to the hydrophobic nature of carboxymethyl chitosan and polyphenolic compounds present in the extract. The addition of CCSE 0.5% slightly reduced the WVP of the CG film ($p < 0.05$), but the WVP varied significantly ($p < 0.05$) for the CG-CCSE 2% film compared with that of the CG control film. The reduction could be linked to the less interactivity between the molecules of the water existing in the film following the effect of the cross-linking between glycerol, CG and CCSE, thereby promoting lower free water availability [52]. For food packaging films, low WVP values are very critical for preventing the transfer of moisture between food and the environment. It has been reported that the addition of polyphenols significantly reduced the WVP of sodium alginate/gum Arabic-based films [32]. Similar behavior was also documented as a result of the integration of the extract from black and blueberry into CG-based films [53].

### Color and Opacity

The color and opacity of food packaging material are integral indicators for consumer preference. All the variables were influenced ($p < 0.05$) by CCSE (Table 4). The control films were extremely transparent while the color change was observed in the treated groups. A remarkable difference ($p < 0.05$) was recorded between all color indicator values ($L^*$, $a^*$, and $b^*$). The color of the film became extra light amber in CG-CCSE 2 group (Fig. 1C). Film opacity also became higher ($p < 0.05$) by increasing CCSE concentration, making the films more opaque. Transparency in the film network is relevant to polymer alignment. The CG film was extremely transparent in comparison to the CG-CCSE film while the decrease in transparency was dose-dependent. The intermolecular bonding happened by CG and CCSE might be linked as the probable cause. The improvement in the characteristics of color and lowering the tendency of transparency in CG-CCSE films could be beneficial to protect food against color change, nutrient loss and off-flavor [54].

**Table 4** Color and opacity of CG-base films with different concentrations of CCSE

| Film sample | L* | a* | b* | ΔE | YI | WI | Opacity ($mm^{-1}$) |
|---|---|---|---|---|---|---|---|
| CG | $84.98 \pm 0.43^{a}$ | $-1.15 \pm 0.03^{c}$ | $3.40 \pm 0.49^{d}$ | $9.19 \pm 0.43^{d}$ | $5.72 \pm 0.06^{d}$ | $84.56 \pm 0.41^{a}$ | $1.16 \pm 0.07^{d}$ |
| CG-CCSE 0.5 | $71.45 \pm 1.05^{b}$ | $4.22 \pm 0.44^{b}$ | $12.04 \pm 0.32^{c}$ | $24.37 \pm 1.16^{c}$ | $24.09 \pm 0.96^{c}$ | $68.72 \pm 1.13^{b}$ | $10.43 \pm 0.42^{c}$ |
| CG-CCSE 1.2 | $66.84 \pm 0.89^{c}$ | $5.35 \pm 0.24^{a}$ | $22.73 \pm 0.14^{b}$ | $33.38 \pm 0.55^{b}$ | $48.60 \pm 0.38^{b}$ | $59.43 \pm 0.55^{c}$ | $13.76 \pm 0.23^{b}$ |
| CG-CCSE 2 | $65.63 \pm 0.19^{c}$ | $6.22 \pm 0.28^{a}$ | $25.10 \pm 0.02^{a}$ | $35.84 \pm 0.20^{a}$ | $54.64 \pm 0.16^{a}$ | $56.98 \pm 0.19^{d}$ | $21.59 \pm 1.24^{a}$ |

Values are expressed as mean ± standard deviation. Different letters in the same column indicate significant differences ($p < 0.05$)

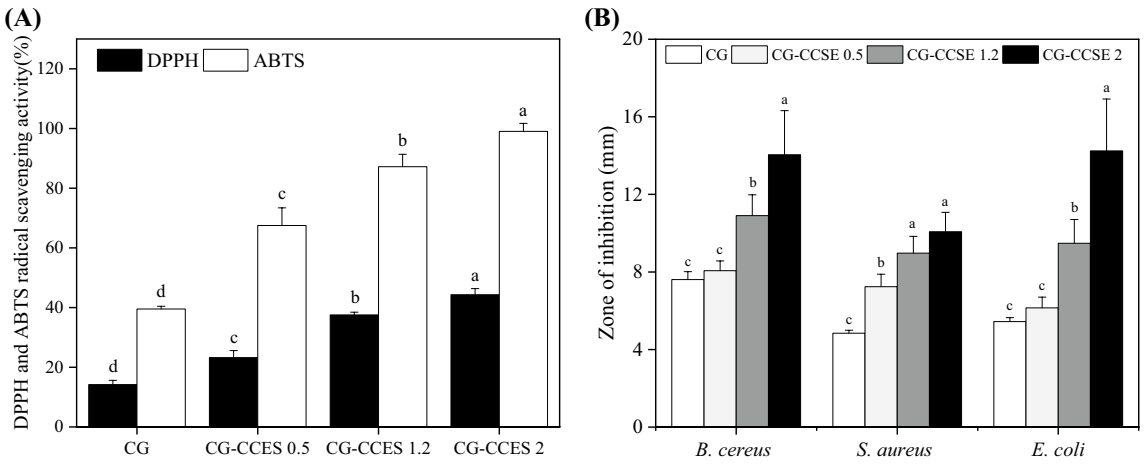


**Fig. 4** **A** Scavenging activities of the CG-CCSE films on ABTS and DPPH radicals, **B** Inhibitory effects of CG-based film with different concentrations CCSE on four kinds of bacteria. Values are mean ± SD ($n = 3$), a-d represent significant differences ($p < 0.05$)

## CG-CCSE Film Bioactivities

### Antioxidant Activity

The assays for DPPH and ABTS free radical scavenging activity were used to evaluate the antioxidant activity of the CG-based composite films and the results are shown in Fig. 4A. The CG control film exhibited negligible antioxidant activity as the DPPH and ABTS scavenging activities were 14% and 39%, respectively. On the contrary, CG-CCSE-based composite films showed a significant increase in antioxidant activity depending on bioactive compounds from *C. camphora* seed extract. The DPPH and ABTS scavenging activities of the CG-CCSE 0.5 composite film slightly increased to 23% and 67%, respectively. When adding more *C. camphora* seed extract (2%), they increased significantly to 44% and 99%, respectively. Therefore, the increase in the total phenolic contents was dose-dependent. Similarly, citric acid also acted as an antioxidant indirectly by chelating effect. The excellent antioxidant activity of CCSE relies on the H-atom donation of the phenolic group of *C. camphora* seed extract [29]. The antioxidant activity of the phenolic groups was contributed by the phenolic ring that can delocalize unpaired electrons and donate hydrogen from the hydroxyl groups [55]. Ounkaew et al. [56] reported that the DPPH scavenging activity of polyvinyl alcohol/starch film increased with increasing citric acid content. A similar result was also reported for an increase in antioxidant activity of biopolymer films incorporated with black soybean seed coat extracts of Pistacia *terebinthus* [35, 57].

### Antimicrobial Activity

The CG-CCSE films demonstrated an inhibitory effect ($p < 0.05$) on both Gram-negative (*E. coli*) and Gram-positive (*S. aureus* and *B. cereus*) bacteria, and the inhibitory zones increased with increasing CCSE concentration in CG (Fig. 4B). The antimicrobial impact of CG films was attributed to high cellular permeability from bacterial cells and CG interaction. Snoussi et al. [58] asserted that the antimicrobial potential of an organic acid with phenolic compounds was linked to the physiological changes occurring in the bacterial membrane, ultimately resulting in cell death [59]. Moreover, citric acid present in CCSE might be involved in the reaction between thiosulfinates and thiol groups, resulting in the inactivation of thiolic enzymes present in Gram-negative bacteria and allyl-disulfide production, which further modified L-cysteine causing bacterial cell death [60]. Therefore, active packaging films should possess significant antimicrobial properties high enough to inhibit microbial growth and enhance the shelf life of foods [61].

### Biodegradation

The biodegradable results of CG and CG-CCSE films are presented in Fig. 5. There was a significant ($p < 0.05$) weight loss in CG-CCSE films as the days progressed. The CG-CCSE 0.5 film showed the maximum loss in weight recorded about 44.77% after 3 weeks (Fig. 5A), whilst the lowest value (34.14%) occurred in the control film (Fig. 5B). A similar biodegradation result was reported when root extract [43] and rosemary extracts [62] were incorporated into the

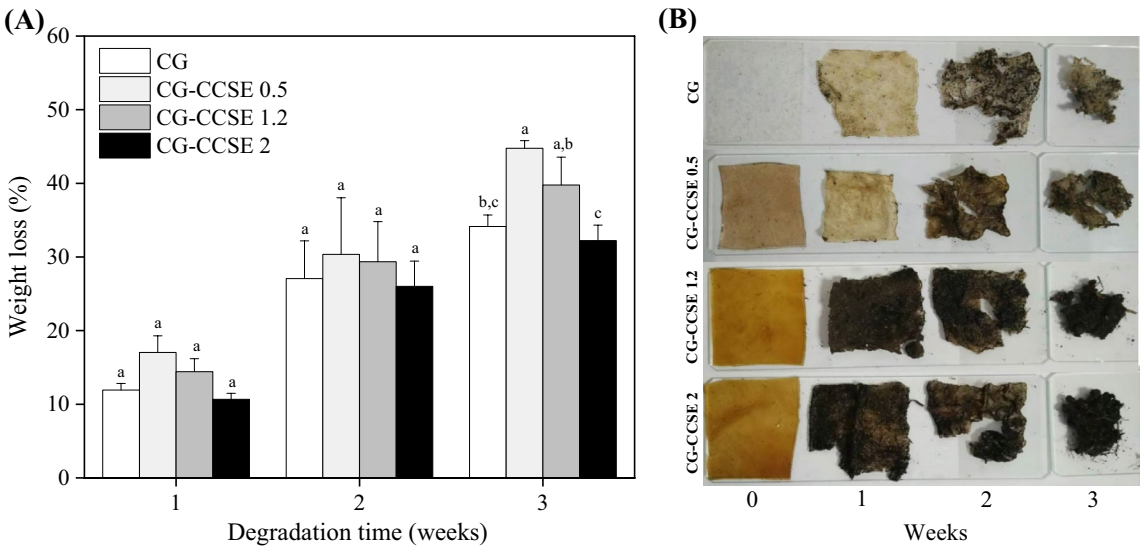


**Fig. 5** **A** Biodegradability evaluation of CG-CCSE films. **B** Photographs of CG-CCSE films during the biodegradation test. Values are mean ± SD ($n = 3$), a-d represent significant differences ($p < 0.05$)

cassava-starch film. The result showed that the CCSE incorporation enhanced Biodegradation following the generation of new polymeric materials, reducing adverse environmental impact by rapid regression.

## Potential Application on Sunflower Oil Packaging

### Capability of Films for Oil Resistance

To ascertain the oil-resistant capability of the films, the oil absorption ratio (OAR) was assessed. The results showed no significant ($p > 0.05$) effect among the treated films. But between the CG- CCSE films and the CG control film, the OAR varied significantly ($p < 0.05$). Films (CG-CCSE 1.2 and 2) exhibited the lowest OAR ($0.13 \pm 0.087$ and $0.08 \pm 0.038$), respectively, while the highest ($0.39 \pm 0.023$) value was observed in CG control film (Table 5). The probable cause could be attributed to the existence of hydrophilic hydroxyl groups in the structure of CG and homogeneity in the structures without bubbles or pores of the films from CCSE inclusion, preventing the permeability of oil molecules out of the films. The low OAR value, therefore, demonstrated a more remarkable ability for oil resistance, which is an essential characteristic for oil products packaging material.

### Peroxide Value (POV)

POV is considered a parameter for producing lipid oxidation primary products (hydroperoxides) [63]. Although all POV values increased as days progressed, as presented in Table 5, the oxidation of CG-CCSE films was markedly ($p < 0.05$) reduced with open and CG controls observed with the highest values ($69.49 \pm 0.68$ and $20.15 \pm 0.31$ mEq/kg, respectively), while the lowest value ($9.79 \pm 0.28$ mEq/kg) was recorded in CG-CCSE 2. Simultaneously, the color changes and oxidation of oils were detected by naked eyes when kept at 50 °C for 28 days (as shown graphically in Fig. 6). The higher POV of sunflower oil for the CG film might be a result of the discontinuities in the matrix of the CG film (Fig. 1A), which would permit accelerated oil oxidation. The high level of unsaturated fatty acids in the oil and direct exposure to external oxygen could be probable causes. The compacted structure of the bio-composite film showed an integral part in reducing oxidation by making oxygen impermeable [9, 64]. The slow release of the citric acid from the CG-CCSE was probably proficient to improve the balance of citric acid and retard the oxidation process of the sunflower oil during preservation [56]. Besides, the antioxidant potency of the film following the availability of citric acid and polyphenols also induced the retardation of the oxidative processes. Therefore, it can be concluded that

**Table 5** Oil absorption ratio (OAR %) of CG-CCSE films and POV (mEq/kg) of sunflower oil stored in CG-CCSE films

| Film sample | OAR | POV | | | | |
|---|---|---|---|---|---|---|
| | | Day 1 | Day 7 | Day 14 | Day 21 | Day 28 |
| Open control | – | $2.83 \pm 0.20^{a}$ | $8.01 \pm 0.20^{a}$ | $22.00 \pm 0.54^{a}$ | $41.03 \pm 0.47^{a}$ | $69.49 \pm 0.68^{a}$ |
| CG | $0.39 \pm 0.023^{a}$ | $2.64 \pm 0.22^{a}$ | $6.67 \pm 0.24^{b}$ | $10.48 \pm 0.48^{b}$ | $15.64 \pm 0.68^{b}$ | $20.15 \pm 0.31^{b}$ |
| CG-CCSE 0.5 | $0.19 \pm 0.066^{b}$ | $2.63 \pm 0.24^{a}$ | $6.19 \pm 0.17^{b}$ | $9.76 \pm 0.24^{b}$ | $14.36 \pm 0.51^{b}$ | $17.36 \pm 0.46^{b, c}$ |
| CG-CCSE 1.2 | $0.13 \pm 0.087^{b}$ | $2.66 \pm 0.26^{a}$ | $4.93 \pm 0.00^{c}$ | $7.78 \pm 0.27^{c}$ | $10.46 \pm 0.26^{c}$ | $15.13 \pm 2.16^{c}$ |
| CG-CCSE 2 | $0.08 \pm 0.038^{b}$ | $2.63 \pm 0.19^{a}$ | $4.33 \pm 0.24^{d}$ | $6.76 \pm 0.56^{c}$ | $7.69 \pm 0.00^{d}$ | $9.79 \pm 0.28^{d}$ |

Values are expressed as mean ± standard deviation. Different letters in the same column indicate significant differences ($p < 0.05$)


**Fig. 6** Photographs of uncovered, CG, CG-CCSE 0.5, CG-CCSE 1.2 and CG-CCSE 2 films during the oxidation and rancidity of sunflower oil caused after sealed and stored at 50 °C for 28 days

CG-based CCSE films, possessing good bioactive properties, can be used for active packaging applications to prevent oxidation and deterioration of food.

## Conclusion

*C. camphora* seed extract, which is regarded as food waste, possesses rich bioactive compounds such as citric acid, 4-hydroxybenzoic acid, and other phenolic compounds, which can be explored as a potential packaging alternative. In this study, CG-based multifunctional composite films were prepared by incorporating CCSE using a solution casting method. The addition of CCSE affected the physical and functional properties of the prepared CG-based composite films. The SEM, FT-IR, XRD and DSC results showed that CCSE was uniformly dispersed in the biopolymer matrix to make compatible composite films. The addition of CCSE (1.2 and 2.0%) improved film properties such as mechanical, water solubility, moisture content, swelling degree, water vapor barrier properties, transparency and opacity. CG-CCSE 2 composite film showed the highest mechanical properties, while the CG-CCSE 1.2 composite film showed the highest biodegradability. CG-CCSE 2 composite film exhibited high antioxidant activity and strong antibacterial activity against foodborne pathogenic bacteria, *S. aureus*, *B. cereus* and *E. coli*. The CG-based films, such as CG-CCSE 2, are most likely to be used as active food packaging for preventing lipid oxidation, ensuring food safety and extending the shelf life of packaged foods.

**Acknowledgements** This work was supported by a project funded by the Priority Academic Program Development of Jiangsu Higher Education Institutions.

**Author Contributions** FA: Conceptualization, Software, Writing original draft. APB: Investigation. MA: Methodology, Data Curation. MAS: Investigation. MMN: Investigation. ZD: Investigation. YH: Investigation. XZ: Conceptualization, Supervision, Funding, Project administration.

## Declarations

**Conflict of Interest** The authors have declared that there is no conflict of interest.

## References

1. Cox KD, Covernton GA, Davies HL, Dower JF, Juanes F, Dudas SE (2019) Human consumption of microplastics. Environm Sci Technol 53(12):7068–7074
2. Hassan B, Chatha SAS, Hussain AI, Zia KM, Akhtar N (2018) Recent advances on polysaccharides, lipids and protein based edible films and coatings: a review. Int J Biol Macromol 109:1095–1107
3. Otoni CG, Avena-Bustillos RJ, Azeredo HM, Lorevice MV, Moura MR, Mattoso LH et al (2017) Recent advances on edible films based on fruits and vegetables—a review. Compr Rev Food Sci Food Saf 16(5):1151–1169
4. Akhtar HMS, Riaz A, Hamed YS, Abdin M, Chen G, Wan P et al (2018) Production and characterization of CMC-based antioxidant and antimicrobial films enriched with chickpea hull polysaccharides. Int J Biol Macromol 118:469–477
5. Adilah AN, Jamilah B, Noranizan M, Hanani ZN (2018) Utilization of mango peel extracts on the biodegradable films for active packaging. Food Packag Shelf Life 16:1–7
6. Asdagh A, Karimi Sani I, Pirsa S, Amiri S, Shariatifar N, Eghbaljoo-Gharehgheshlaghi H et al (2021) Production and characterization of nanocomposite film based on whey protein isolated/copper oxide nanoparticles containing coconut essential oil and paprika extract. J Polym Environ 29(1):335–349
7. Jabraili A, Pirsa S, Pirouzifard MK, Amiri S (2021) Biodegradable nanocomposite film based on gluten/silica/calcium chloride: physicochemical properties and bioactive compounds extraction capacity. J Polym Environ 29(8):2557–2571
8. Medina-Jaramillo C, Ochoa-Yepes O, Bernal C, Famá L (2017) Active and smart biodegradable packaging based on starch and natural extracts. Carbohydr Polym 176:187–194
9. Riaz A, Lagnika C, Luo H, Dai Z, Nie M, Hashim MM et al (2020) Chitosan-based biodegradable active food packaging film containing Chinese chive (*Allium tuberosum*) root extract for food application. Int J Biol Macromol 150:595–604
10. Ciannamea EM, Stefani PM, Ruseckaite RA (2016) Properties and antioxidant activity of soy protein concentrate films incorporated with red grape extract processed by casting and compression molding. LWT Food Sci Technol 74:353–362
11. Gómez-Estaca J, López-de-Dicastillo C, Hernández-Muñoz P, Catalá R, Gavara R (2014) Advances in antioxidant active food packaging. Trends Food Sci Technol 35(1):42–51
12. Shariatinia Z (2018) Carboxymethyl chitosan: properties and biomedical applications. Int J Biol Macromol 120:1406–1419
13. Ali A, Maqbool M, Ramachandran S, Alderson PG (2010) Gum arabic as a novel edible coating for enhancing shelf-life and improving postharvest quality of tomato (Solanum lycopersicum L.) fruit. Postharvest Biol Technol 58(1):42–47
14. Abdin M, Salama MA, Gawad R, Fathi MA, Alnadari F (2021) Two-steps of gelation system enhanced the stability of Syzygium cumini anthocyanins by encapsulation with sodium alginate, maltodextrin, chitosan and gum Arabic. J Polym Environ 29:3679–3692
15. Ghasemizad S, Pirsa S, Amiri S, Abdosatari P (2022) Optimization and characterization of bioactive biocomposite film based onorange peel incorporated with gum Arabic reinforced by $Cr_2O_3$ nanoparticles. J Polym Environ. https://doi.org/10.1007/s10924-021-02357-2
16. Xu C, Feng X, Huang M, Yang Y, Shen X, Tang X (2019) Cinnamon and clove essential oils to improve physical, thermal and antimicrobial properties of chitosan-gum arabic polyelectrolyte complexed films. Carbohydr Polym 217:116–125
17. Huang G-Q, Du Y-L, Xiao J-X, Wang G-Y (2017) Effect of coacervation conditions on the viscoelastic properties of N, O-carboxymethyl chitosan–gum Arabic coacervates. Food Chem 228:236–242
18. Zimet P, Mombrú ÁW, Mombrú D, Castro A, Villanueva JP, Pardo H et al (2019) Physico-chemical and antilisterial properties of nisin-incorporated chitosan/carboxymethyl chitosan films. Carbohydr Polym 219:334–343
19. Bai R, Zhang X, Yong H, Wang X, Liu Y, Liu J (2019) Development and characterization of antioxidant active packaging and

intelligent $Al^{3+}$-sensing films based on carboxymethyl chitosan and quercetin. Int J Biol Macromol 126:1074–1084
20. Suriyatem R, Auras RA, Rachtanapun C, Rachtanapun P (2018) Biodegradable rice starch/carboxymethyl chitosan films with added propolis extract for potential use as active food packaging. Polymers 10(9):954
21. Wu J, Zhong F, Li Y, Shoemaker C, Xia W (2013) Preparation and characterization of pullulan–chitosan and pullulan–carboxymethyl chitosan blended films. Food Hydrocoll 30(1):82–91
22. Ribeiro AM, Estevinho BN, Rocha F (2020) Edible films prepared with different biopolymers, containing polyphenols extracted from Elderberry (Sambucus Nigra L.), to protect food products and to improve food functionality. Food Bioprocess Technol 13(10):1742–1754
23. Tahsiri Z, Mirzaei H, Hosseini SMH, Khalesi M (2019) Gum arabic improves the mechanical properties of wild almond protein film. Carbohydr Polym 222:114994
24. Muppalla SR, Chawla S (2018) Effect of gum Arabic-polyvinyl alcohol films containing seed cover extract of Zanthoxylum rhetsa on shelf life of refrigerated ground chicken meat. J Food Saf 38(4):e12460
25. Zhang G, Yan X, Wu S, Ma M, Yu P, Gong D et al (2020) Ethanol extracts from *Cinnamomum camphora* seed kernel: potential bioactivities as affected by alkaline hydrolysis and simulated gastrointestinal digestion. Food Res Int 137:109363
26. Fu J, Zeng C, Zeng Z, Wang B, Gong D (2016) Cinnamomum camphora seed kernel oil ameliorates oxidative stress and inflammation in diet-induced obese rats. J Food Sci 81(5):H1295–H1300
27. Yan X, Liang S, Peng T, Zhang G, Zeng Z, Yu P et al (2020) Influence of phenolic compounds on physicochemical and functional properties of protein isolate from *Cinnamomum camphora* seed kernel. Food Hydrocoll 102:105612
28. Guo S, Geng Z, Zhang W, Liang J, Wang C, Deng Z et al (2016) The chemical composition of essential oils from *Cinnamomum camphora* and their insecticidal activity against the stored product pests. IJMS 17(11):1836
29. Liu C-M, Perng M-H, Chen C-Y (2018) Antioxidant activities of crude extracts from peel and seed of Cinnamomum camphora. Biomed Res 29(13):2854–2858
30. Islam E, Islam R, Rahman AA, Alam AK, Khondkar P, Rashid M et al (2013) Estimation of total phenol and in vitro antioxidant activity of Albizia procera leaves. BMC Res notes 6(1):1–7
31. Zhang P, Zhao Y, Shi Q (2016) Characterization of a novel edible film based on gum ghatti: effect of plasticizer type and concentration. Carbohydr Polym 153:345–355
32. Abdin M, El-Beltagy A, El-sayed M, Naeem MA (2021) Production and characterization of sodium alginate/Gum Arabic based films enriched with Syzygium cumini seeds extracts for food application. J Polym Environ 30:1615–1626
33. Khalid S, Yu L, Feng M, Meng L, Bai Y, Ali A et al (2018) Development and characterization of biodegradable antimicrobial packaging films based on polycaprolactone, starch and pomegranate rind hybrids. Food Packag Shelf Life 18:71–79
34. Tan Z, Yi Y, Wang H, Zhou W, Yang Y, Wang C (2016) Physical and degradable properties of mulching films prepared from natural fibers and biodegradable polymers. Appl Sci 6(5):147
35. Wang X, Yong H, Gao L, Li L, Jin M, Liu J (2019) Preparation and characterization of antioxidant and pH-sensitive films based on chitosan and black soybean seed coat extract. Food Hydrocoll 89:56–66
36. General Administration of Quality Supervision Inspection and Quarantine of the People's Republic of China (2016) National standards of the People's Republic of China.
37. Kang S, Xiao Y, Guo X, Huang A, Xu HJFC (2021) Development of gum arabic-based nanocomposite films reinforced with cellulose nanocrystals for strawberry preservation. Food Chem 350:129199
38. Roy S, Rhim J-W (2020) Carboxymethyl cellulose-based antioxidant and antimicrobial active packaging film incorporated with curcumin and zinc oxide. Int J Biol Macromol 148:666–676
39. Cheng S-Y, Wang B-J, Weng Y-M (2015) Antioxidant and antimicrobial edible zein/chitosan composite films fabricated by incorporation of phenolic compounds and dicarboxylic acids. LWT Food Sci Technol 63(1):115–121
40. Dou L, Li B, Zhang K, Chu X, Hou H (2018) Physical properties and antioxidant activity of gelatin-sodium alginate edible films with tea polyphenols. Int J Biol Macromol 118:1377–1383
41. Lawrie G, Keen I, Drew B, Chandler-Temple A, Rintoul L, Fredericks P et al (2007) Interactions between alginate and chitosan biopolymers characterized using FTIR and XPS. Biomacromol 8(8):2533–2541
42. Wang H, Gong X, Miao Y, Guo X, Liu C, Fan Y-Y et al (2019) Preparation and characterization of multilayer films composed of chitosan, sodium alginate and carboxymethyl chitosan-ZnO nanoparticles. Food Chem 283:397–403
43. Riaz A, Lagnika C, Luo H, Nie M, Dai Z, Liu C et al (2020) Effect of Chinese chives (*Allium tuberosum*) addition to carboxymethyl cellulose based food packaging films. Carbohydr Polym 235:115944
44. Martins JT, Cerqueira MA, Vicente AA (2012) Influence of α-tocopherol on physicochemical properties of chitosan-based films. Food Hydrocoll 27(1):220–227
45. Wang S, Xia P, Wang S, Liang J, Sun Y, Yue P et al (2019) Packaging films formulated with gelatin and anthocyanins nanocomplexes: physical properties, antioxidant activity and its application for olive oil protection. Food Hydrocoll 96:617–624
46. Kang S, Xiao Y, Guo X, Huang A, Xu H (2021) Development of gum arabic-based nanocomposite films reinforced with cellulose nanocrystals for strawberry preservation. Food Chem 350:129199
47. Qin Y, Liu Y, Yong H, Liu J, Zhang X, Liu J (2019) Preparation and characterization of active and intelligent packaging films based on cassava starch and anthocyanins from Lycium ruthenicum Murr. Int J Biol Macromol 134:80–90
48. Pastor C, Sánchez-González L, Chiralt A, Cháfer M, González-Martínez C (2013) Physical and antioxidant properties of chitosan and methylcellulose based films containing resveratrol. Food Hydrocoll 30(1):272–280
49. Hosseini SF, Rezaei M, Zandi M, Farahmandghavi F (2016) Development of bioactive fish gelatin/chitosan nanoparticles composite films with antimicrobial properties. Food Chem 194:1266–1274
50. Uranga J, Puertas A, Etxabide A, Dueñas M, Guerrero P, De La Caba K (2019) Citric acid-incorporated fish gelatin/chitosan composite films. Food Hydrocoll 86:95–103
51. Rui L, Xie M, Hu B, Zhou L, Yin D, Zeng X (2017) A comparative study on chitosan/gelatin composite films with conjugated or incorporated gallic acid. Carbohydr Polym 173:473–481
52. Siripatrawan U, Harte BR (2010) Physical properties and antioxidant activity of an active film from chitosan incorporated with green tea extract. Food Hydrocoll 24(8):770–775
53. Bifani V, Ramírez C, Ihl M, Rubilar M, García A, Zaritzky N (2007) Effects of murta (Ugni molinae Turcz) extract on gas and water vapor permeability of carboxymethylcellulose-based edible films. Lebensm Wiss Technol 40(8):1473–1481
54. Arfat YA, Ahmed J, Hiremath N, Auras R, Joseph A (2017) Thermo-mechanical, rheological, structural and antimicrobial properties of bionanocomposite films based on fish skin gelatin and silver-copper nanoparticles. Food Hydrocoll 62:191–202

55. Palacios I, Lozano M, Moro C, D'arrigo M, Rostagno M, Martínez J et al (2011) Antioxidant properties of phenolic compounds occurring in edible mushrooms. Food Chem 128(3):674–678
56. Ounkaew A, Kasemsiri P, Kamwilaisak K, Saengprachatanarug K, Mongkolthanaruk W, Souvanh M et al (2018) Polyvinyl alcohol (PVA)/starch bioactive packaging film enriched with antioxidants from spent coffee ground and citric acid. J Polym Environ 26(9):3762–3772
57. Kaya M, Khadem S, Cakmak YS, Mujtaba M, Ilk S, Akyuz L et al (2018) Antioxidative and antimicrobial edible chitosan films blended with stem, leaf and seed extracts of Pistacia terebinthus for active food packaging. RSC Adv 8(8):3941–3950
58. Snoussi M, Trabelsi N, Dehmeni A, Benzekri R, Bouslama L, Hajlaoui B et al (2016) Phytochemical analysis, antimicrobial and antioxidant activities of Allium roseum var. odoratissimum (Desf.) coss extracts. Ind Crop Prod 89:533–542
59. Ali A, Chen Y, Liu H, Yu L, Baloch Z, Khalid S et al (2019) Starch-based antimicrobial films functionalized by pomegranate peel. Int J Biol Macromol 129:1120–1126
60. Hussain G, Rahman A, Hussain T, Uddin S, Ali T (2015) Citric and lactic acid effects on the growth Inhibition of E. coli and S. typhymurium on beef during storage. Sarhad J Agric 31(3):183–190
61. Wu Y, Luo X, Li W, Song R, Li J, Li Y et al (2016) Green and biodegradable composite films with novel antimicrobial performance based on cellulose. Food Chem 197:250–256
62. Piñeros-Hernandez D, Medina-Jaramillo C, López-Córdoba A, Goyanes S (2017) Edible cassava starch films carrying rosemary antioxidant extracts for potential use as active food packaging. Food Hydrocoll 63:488–4895
63. Salama MA, El Harkaoui S, Nounah I, Sakr H, Abdin M, Owon M et al (2020) Oxidative stability of Opuntia ficus-indica seeds oil blending with Moringa oleifera seeds oil. OCL 27:53
64. Asadzadeh F, Pirsa S (2021) Zein/EDTA/chlorophyll/nano-clay biocomposite sorbent: Investigation physicochemical properties sorbent and its ability to remove contaminants of industrial wastewater. J Polym Environ. https://doi.org/10.1007/s10924-021-02328-7

**Publisher's Note** Springer Nature remains neutral with regard to jurisdictional claims in published maps and institutional affiliations.